Optical Conductivity of High T_c Superconductors: From Underdoped to Overdoped

A. V. Puchkov,[1] P. Fournier,[2,*] T. Timusk,[1] and N. N. Kolesnikov[3]
[1]*Department of Physics and Astronomy, McMaster University, Hamilton, Ontario, Canada L8S4M1*
[2]*Edward L. Ginzton Laboratory, Stanford University, Stanford, California 94305*
[3]*Institute of Solid State Physics, Chernogolovka, Russia 142432*
(Received 12 April 1996)

We present results of room-temperature reflectivity measurements on overdoped Tl2201 and on underdoped and overdoped Bi2212 single crystals. The optical conductivity $\sigma(\omega)$ has two distinctly different regimes as a function of doping. While in the underdoped regime the doping-induced changes in $\sigma(\omega)$ can be well described by an increasing density of mobile carriers, in the overdoped regime there is no evidence for such an increase. Our results are not consistent with the usual view on the overdoped regime where reduction of T_c is associated with an increase in the density of mobile charge carriers. [S0031-9007(96)01026-5]

PACS numbers: 74.62.Dh, 74.25.Fy, 74.25.Gz

One of the most unusual features of the high T_c (HTSC) phenomenon is the peculiar dependence of the superconducting transition temperature T_c on the doping level. It is customary to divide the phase diagram of HTSC into three different regimes: (1) the "underdoped" regime, where the superconducting phase is adjacent to the insulating phase and T_c increases with increasing (p-type) doping; (2) the "optimum" T_c regime, where T_c reaches the highest value within a given series; and (3) the "overdoped" regime where T_c decreases with further doping while the material becomes a better metal.

While the underdoped and optimally doped regimes have been studied extensively, the overdoped regime has not enjoyed this kind of attention. It is generally believed that the decrease of T_c with overdoping is associated with an increasing concentration of mobile carriers (holes). For example, a "universal" dependence $T_c(p)$, where p is a number of holes per planar Cu, was suggested where T_c reduces parabolically with p for $p > 0.16$ (overdoped regime) [1,2]. If true, this behavior is most unusual and surprising, since in the conventional superconductors an increased carrier density normally leads to an *increased* T_c.

The main purpose of this study is to determine whether or not this view on overdoped HTSC is consistent with the experimental results on the optical conductivity. We present, for the first time, a systematic study of the optical conductivity in the whole doping range from underdoped to overdoped. Our study reveals that while in the underdoped regime progressive doping indeed increases the free-carrier density, this trend does not continue to the overdoped part of the phase diagram.

Infrared reflectance spectroscopy is an effective tool for studying electron dynamics as it allows one to obtain the frequency-dependent dielectric constants and therefore the spectrum of electronic excitations in the energy range characteristic for conducting carriers. Information about mobile carrier density can be obtained from the spectral weight (SW) contained by the low-frequency real part of optical conductivity $\sigma_1(\omega)$. An effective density of carriers contributing to optical transitions below a certain cutoff energy $\hbar\omega_0$, $n_{eff}(\omega_0)$, is given by a SW of $\sigma_1(\omega)$, integrated over energies from zero to $\hbar\omega_0$ [3]:

$$n_{eff}(\omega_0) = \frac{m_e}{8\pi e^2} \int_0^{\omega_0} \sigma_1(\omega)\, d\omega\,, \qquad (1)$$

where m_e is a bare electron mass.

To obtain the real and imaginary parts of optical conductivity we have performed reflectivity measurements on $Bi_2Sr_2CaCu_2O_{8+\delta}$ (Bi2212) and $Tl_2Ba_2CuO_{6+\delta}$ (Tl2201) single crystals at several doping levels. Three Bi2212 single crystals with $T_c = 67$ K, 82 K (both underdoped) and $T_c = 82$ K (overdoped) were measured. The Bi2212 crystals were prepared from the as-grown crystals by annealed in argon and/or oxygen. The three T2201 single crystals used in the measurements had T_c's of 90 K (highest T_c achievable), 60 K and 23 K (both overdoped).

The real part of the optical conductivity $\sigma_1(\omega)$ was calculated using Kramers-Kronig (KK) analysis of reflectivity. For the KK calculations the reflectivity was approximated by a constant value from the upper limit of our measurements 40 000 cm^{-1} (5 eV) to 300 000 cm^{-1}, where reflectivity was allowed to fall as ω^{-4}. Below 30 cm^{-1} the Hagen-Rubens formula, with parameters taken from the dc resistivity measurements [4,5], was used. Both low- and high-frequency reflectivity approximations were found to have little effect on $\sigma_1(\omega)$ in the energy region studied in this work.

The real part of the optical conductivity for Bi2212 material at three doping levels is shown in Fig. 1 at room temperature. The inset on the lowest panel of Fig. 1 shows the difference between $\sigma_1(\omega)$ obtained for the $T_c = 82$ K slightly overdoped sample (upper panel) and the $T_c = 67$ K underdoped sample (lower panel) [6]. First, the low-frequency conductivity SW increases with doping in the underdoped regime. Second, the differential conductivity spectrum has a Lorentzian (Drude-like) shape characteristic for a free-carrier absorption [3,7].

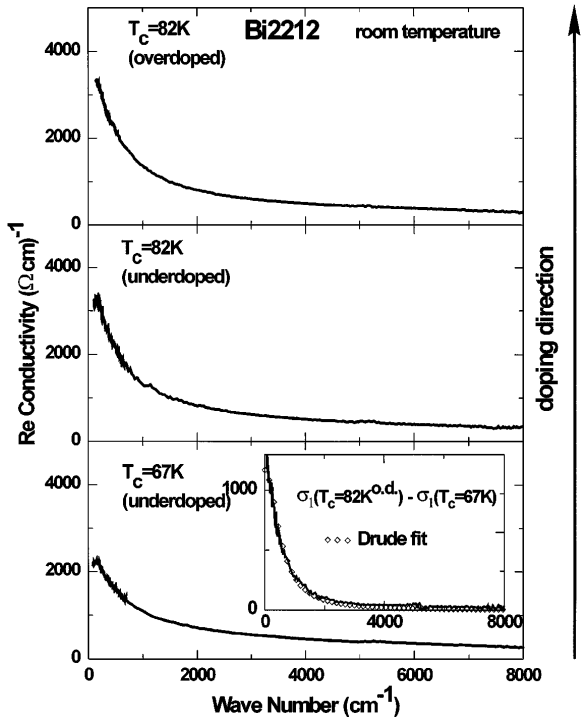

FIG. 1. The optical conductivity of Bi2212 at several doping levels. Inset: solid line is the difference between $\sigma_1(\omega)$ shown in the upper panel and $\sigma_1(\omega)$ shown in the lower panel. The open symbols represent a fit by a Drude form.

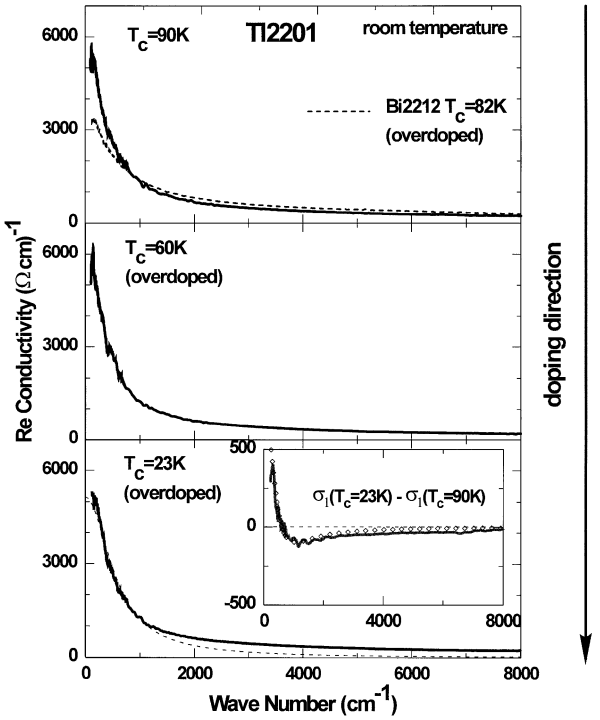

FIG. 2. The optical conductivity of Tl2201 at several doping levels. On the upper panel $\sigma_1(\omega)$ for slightly overdoped Bi2212 is shown for comparison. On the lower panel a Drude curve with $\omega_p = 13\,000$ cm^{-1} and $1/\tau = 560$ cm^{-1} is shown for illustration as described in text. Inset: solid line is the difference between $\sigma_1(\omega)$ for the $T_c = 23$ and 90 K samples. The open symbols show a fit to the difference of two Drude curves with the same ω_p but different $1/\tau$ as described in the text.

The Drude-like shape of the differential conductivity suggests that it is a difference of two spectra that contain free-carrier contributions with similar scattering rates $1/\tau$ but different plasma frequencies (larger for the more heavily doped sample). The increase in the plasma frequency of the Drude part is consistent with the scenario where doping in the underdoped regime produces additional mobile carriers [8]. One can also see from the inset of Fig. 1 that the increase of the low-frequency SW with doping in the underdoped regime is confined to the energy range below 1 eV [9]. We note that the doping-induced conductivity increase was found to be confined to below 1 eV in metallic $YBa_2Cu_3O_{7-\delta}$ as well [8].

The $\sigma_1(\omega)$ in the overdoped regime is shown in Fig. 2 for the Tl2201 system at three doping levels, from the one with the highest T_c achievable (90 K) to the strongly overdoped one with $T_c = 23$ K. The inset in the lowest panel shows the difference between $\sigma_1(\omega)$ for the $T_c = 23$ and 90 K samples. The resulting differential spectrum is qualitatively different from the one obtained for Bi2212: now there is no doping-induced increase in the conductivity SW. Instead, the SW is *redistributed* with part of it moved from the midinfrared frequencies to the lower frequencies with (over)doping. This behavior is reminiscent to what was observed by Tamasaku *et al.* in the $La_{2-x}Sr_xCuO_4$ system [10]: Although the transfer of conductivity SW from above the charge-transfer gap is nearly saturated as doping is increased above optimal, the SW is biased towards the lower-energy region with overdoping. Again, the redistribution of the SW occurs in the energy range below 1 eV. The differential spectrum can no longer be fitted to a difference of two spectra containing Drude absorption peaks with the same scattering rates but different plasma frequencies. However, now it has the shape of the difference of two Drude peaks with the same plasma frequency but different scattering rates, as is shown in the inset. The parameters used in the fit were $\omega_p = 13\,000$ cm^{-1}, $1/\tau(T_c = 23\text{ K}) = 560$ cm^{-1}, $1/\tau(T_c = 90\text{ K}) = 660$ cm^{-1}, values not at all unreasonable. For illustration, a Drude peak with $\omega_p = 13\,000$ cm^{-1} and $1/\tau = 560$ cm^{-1} is shown in the bottom panel of Fig. 2.

To make the analysis more quantitative in Fig. 3 we have plotted the SW of the low-frequency ($\hbar\omega_0 = 1$ eV) optical conductivity as a function of T_c. The $\hbar\omega_0 = 1$ eV was chosen to isolate the energy region where the conductivity actually changes with doping in the doping range considered in this work. For reasons described below we will mainly be interested in relative *changes* in the SW as a function of doping as opposed to its absolute values. Therefore, we have normalized our results to those obtained for the optimal doping concentrations within each series. On the horizontal

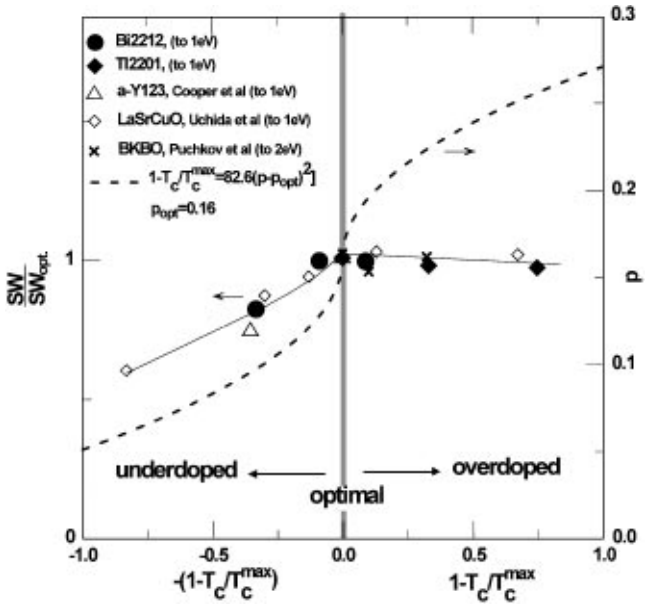

FIG. 3. The relative changes in the low-frequency conductivity spectral weight are plotted for several HTSC material series as a function of T_c. The left-hand part corresponds to underdoped regime, the right-hand part corresponds to the overdoped regime. The dashed line shows a low-frequency spectral weight expected on the basis of parabolic dependence $T_c(p)$ proposed for the HTSC cuprates.

axis we plot T_c in the functional form $\pm(1 - T_c/T_c^{\max})$, with a minus sign for the underdoped materials and plus sign for the overdoped ones. Previously published results for several other cuprate materials are plotted as well [10–12]. We also include data obtained on 3D HTSC material $Ba_{1-x}K_xBiO_3$ at doping levels with $T_c = 31$, 28, and 21 K [13,14]. All of the data points fall on the same curve which is highly asymmetrical with respect to the point of optimal doping $(0, 1)$. While in the underdoped regime an increase in T_c is accompanied by an increase in the low-frequency conductivity SW; this behavior changes abruptly at the optimal doping: in the overdoped regime an increase in the low-frequency SW is not observed. In fact, if it changes at all, it decreases with decreasing T_c.

The results presented above suggest that the optimal doping level is not only the one with the highest T_c in a given series, but it also separates two distinctly different regimes of optical conductivity behavior as a function of doping. While in the underdoped regime the total low-frequency conductivity spectral weight increases with doping, which can be attributed to the increasing density of the mobile charge carriers, in the overdoped regime the total spectral weight below 1 eV does not increase and the changes in $\sigma_1(\omega)$ are more likely to be due to the changing scattering rate of the mobile carriers.

Before we use the finite-energy sum rule analysis to make a connection between the doping dependence of the conductivity SW and the mobile carrier density, we show how despite some of its shortcomings the essential information can be extracted. The HTSC materials demonstrate a complicated non-Drude-shape of $\sigma_1(\omega)$ where the free-carrier absorption is not obviously defined [3]. This makes the choice of $\hbar\omega_0$ ambiguous. There are two approaches to describe the optical conductivity of the HTSC cuprates. The first one is a two-component approach in which the total conductivity is divided into a free-carrier Drude and bound-carrier mid-infrared (MIR) parts, independent of each other. The alternative approach is a one-component one, in which both parts are due to excitations of the same "kind" of charge carriers that have frequency-dependent effective mass and scattering rate. This may result in an intensive conductivity sideband at the MIR frequencies as in the case of metals with strong electron-phonon interaction [15,16]. The SW of the MIR sideband is taken from the Drude absorption so that their *total* SW represents the actual free-carrier density.

It is outside the scope of this Letter to decide which description is the correct one but we can outline the consequences that each of them may have on the analysis of Eq. (1). (i) The two-component model: an integration of Eq. (1) will give an overestimated absolute value of the mobile carrier density as it will include the "parasitic" MIR absorption. However, as the SW of the MIR conductivity does not change very much with doping (see the insets of Figs. 1 and 2), we can still conduct a *comparative* analysis of *changes* in the free carrier density with doping within a given series. (ii) The one-component model: an integration in the range from 0 to 1 eV, which essentially includes both the free-carrier part and the MIR sideband, may in fact give us the absolute value of the free carrier density close to the correct one. However, the MIR absorption may still include, for example, an interband transition. In this case while the absolute values of carrier density obtained using Eq. (1) may be misleading, the comparative analysis still can be conducted.

In the light of the above discussion we believe that the doping-induced *changes* in the low-frequency SW reflect changes in the mobile carrier density. This puts the results presented in Fig. 3 in contradiction with the scenario where a decrease of T_c in the overdoped regime is a consequence, or associated with, the increasing mobile carrier density. For comparison, in Fig. 3 we have plotted the SW expected from the relation $1 - T_c/T_c^{\max} = 82.6(0.16 - p)^2$, proposed as a universal relation for HTSC cuprates [2]. While in the underdoped regime this relation is in qualitative agreement with the experiment (the density of the mobile carriers increases with doping), there is a qualitative difference in the overdoped regime: the experimental free-carrier density is *not* increasing with overdoping [17].

The optical conductivities of Bi2212 double plane and Tl2201 single plane are very similar, the only difference being the bias of the SW towards lower frequencies in Tl2201 (see the upper panel of Fig. 2). This suggests that the 3D densities of mobile charge carriers are similar in both materials. Taking into account corrections for the volume per formula unit makes carrier density *per plane*

50% smaller in Bi2212 than in Tl2201. One may argue that it is not clear if $T_c = 90$ K Tl2201 is optimally doped, as the peak in T_c as a function of doping has not been observed for this material. However, the Bi2212 sample is doped close to optimal. The 50% larger carrier density substituted into the parabolic relation of the previous paragraph would make the $T_c = 90$ K Tl2201 a strongly overdoped material with hypothetical $T_c^{\max} \simeq 190$ K. On the other hand, if $T_c = 90\ \text{K} = T_c^{\max}$ for Tl2201, the whole idea of T_c being determined by the normal-state free-carrier density *per planar Cu* is put in question. One can assume that TlO planes may also be conducting, and therefore contribute to the low-frequency *ab*-plane conductivity SW. However, while theoretical estimates support this possibility, they predict that TlO planes contribute only a small fraction of the total SW [18].

In an attempt to understand why progressive *p*-type doping does not produce a monotonic increase of the free-carrier density we examine how the dc transport properties evolve with doping. It has been reported that the room-temperature thermoelectric power coefficient (TEP) of HTSC cuprates has a universal behavior as a function of doping: it is large and positive in underdoped samples, almost zero in optimally doped samples, and becomes small and negative upon crossing into the overdoped regime [19]. The Hall coefficient R_H is large and positive in the underdoped regime, decreases in magnitude with doping, and crosses zero somewhere in the overdoped regime. It was suggested, in an attempt to explain the doping dependence of R_H in $La_{2-x}Sr_xCuO_4$, that zero crossing may be a result of a change in the topology of Fermi surface from holelike to electronlike [20]. Indeed, the doping dependence of TEP, which in a simple model is negative (positive) for an electronlike (holelike) Fermi surface [7], would support this scenario.

On the other hand, $\sigma_1(\omega)$, unlike TEP and R_H, does not distinguish between the sign of the charge carriers and depends only on their density, that is on the volume of the (holelike or electronlike) Fermi surface. In a simple rigid-band picture the density of *mobile* charge carriers, and therefore the low-frequency conductivity SW, will attain its maximum as a function of doping at the band filling corresponding to a reflection point where inverse effective mass goes to zero. This corresponds to a band filling at which Fermi surface changes its topology from holelike to electronlike as a function of *p*-type doping. Although these arguments are likely to be oversimplified and the rigid-band picture may not be applicable to the HTSC cuprates, the change of topology of the Fermi surface might provide a qualitative explanation for the observed turning point in the conductivity SW behavior as a function of doping. Another interesting implication of this result is that the highest T_c is achieved at the doping concentration corresponding to the highest density of states at the Fermi level. It remains unclear, however, why the scattering rate of the mobile carriers seems to decrease with overdoping.

In summary, our optical results show that, while in the underdoped regime, an increase in the low-frequency conductivity SW provides a clear indication of increase in the free carriers density as T_c is increasing. Overdoping decreases T_c but does not lead to an increase in the conductivity SW. Therefore, *optical conductivity shows no signature of increasing mobile carrier density with overdoping*. The doping-induced changes in $\sigma_1(\omega)$ in the overdoped regime are more consistent with a reduction in the scattering rate of the mobile carriers.

We thank D. N. Basov and I. I. Mazin for valuable discussions. This research was supported in part by the National Science and Engineering Research Council of Canada and by the Canadian Institute for Advanced Research. The Bi2212 samples were prepared and characterized at the Stanford Center for Material Research through the NSF/MRSEC program.

*Present address: Center for Superconductivity Research, University of Maryland, College Park, MD 20742-4111.

[1] M. R. Presland *et al.*, Physics C **176**, 95 (1991).
[2] J. L. Tallon *et al.*, Phys. Rev. B **51**, 12 911 (1995).
[3] T. Timusk and D. B. Tanner, in *Physical Properties of High Temperature Superconductors*, edited by D. M. Ginsberg (World Scientific, Singapore, 1989), Vol. I, p. 339.
[4] C. Kendziora *et al.*, Phys. Rev. B **48**, 3531 (1993).
[5] T. Manako *et al.*, Phys. Rev. B **46**, 11 019 (1992).
[6] The room-temperature $\sigma_1(\omega)$ spectra for underdoped and overdoped $T_c = 82$ K samples are almost identical. Therefore, the differential spectrum for the two underdoped samples will be similar.
[7] N. W. Ashcroft and N. D. Mermin, *Solid State Physics* (Saunders College, Philadelphia, 1976).
[8] Joseph Orenstein *et al.*, Phys. Rev. B **42**, 6342 (1990); L. D. Rotter *et al.*, Phys. Rev. Lett. **67**, 2741 (1991).
[9] The parameters used in the fit were $\Delta\omega_p = 6200\ \text{cm}^{-1}$ and $1/\tau = 550\ \text{cm}^{-1} \ll 1$ eV.
[10] K. Tamasaku *et al.*, Phys. Rev. Lett. **72**, 3088 (1994).
[11] While plotting the results by Tamasaku *et al.* [10] we have used the parabolic $T_c(x)$ relation, obtained for $La_{2-x}Sr_xCuO_4$ [1], to calculate T_c's from x.
[12] S. L. Cooper *et al.*, Phys. Rev. B **47**, 8233 (1993).
[13] We plot BKBO data in the overdoped part of Fig. 3 as it becomes a better metal as T_c decreases. The integration has been done up to $\hbar\omega = 2$ eV.
[14] A. V. Puchkov *et al.*, Phys. Rev. B (to be published).
[15] P. B. Allen, Phys. Rev. B **3**, 305 (1971).
[16] S. V. Shulga *et al.*, Physica C **178**, 266 (1991).
[17] The results of previous transmission measurements on overdoped Bi2212 [4] indicate an increase in the conductivity SW in the frequency region $200-600\ \text{cm}^{-1}$ upon overdoping. Although the authors interpreted it as an increase in the *total* SW, it may be a result of the SW redistribution as in Tl2201.
[18] D. J. Singh and W. E. Pickett, Physica C **203**, 193 (1992).
[19] S. D. Obertelli *et al.*, Phys. Rev. B **46**, 14 928 (1992).
[20] N. P. Ong *et al.*, Phys. Rev. B **35**, 8807 (1987); P. B. Allen *et al.*, Phys. Rev. B **36**, 3926 (1987).